Transcriptomic changes resulting from *STK32B* overexpression identifies pathways potentially relevant to essential tremor

Calwing Liao[1,2], Faezah Sarayloo[1,2], Daniel Rochefort[2], Fulya Akçimen[1,2], Greer S. Diamond[2], Alexandre D. Laporte[2], Dan Spiegelman[2], Qin He[3], Hélène Catoire[2], Patrick A. Dion[2,4], Guy A. Rouleau[1,2,4]

[1]Department of Human Genetics, McGill University, Montréal, Quebec, Canada
[2]Montreal Neurological Institute, McGill University, Montréal, Quebec, Canada.
[3]Department of Biomedical Sciences, Université de Montréal, Montréal, Quebec, Canada
[4]Department of Neurology and Neurosurgery, McGill University, Montréal, Quebec, Canada

Corresponding Author:
Dr. Guy A. Rouleau, MD, PhD, FRCPC, OQ
Department of Neurology and Neurosurgery
McGill University
Montréal, Québec, Canada
H3A 2B4
E-mail: guy.rouleau@mcgill.ca

Keywords: *STK32B*, essential tremor, transcriptome, *FUS,*
Conflict of Interests: All authors report no conflict of interests.
Funding Sources: Canadian Institutes of Health Research

Abstract

Essential tremor (ET) is a common movement disorder that has a high heritability. A number of genetic studies have associated different genes and loci with ET, but few have investigated the biology of any of these genes. *STK32B* was significantly associated with ET in a large GWAS study and was found to be overexpressed in ET cerebellar tissue. Here, we overexpressed *STK32B* in human cerebellar DAOY cells and used an RNA-Seq approach to identify differentially expressed genes by comparing the transcriptome profile of these cells to the one of control DAOY cells. Pathway and gene ontology enrichment identified axon guidance, olfactory signalling and calcium-voltage channels as significant. Additionally, we show that overexpressing *STK32B* affects transcript levels of previously implicated ET genes such as *FUS*. Our results investigate the effects of overexpressed *STK32B* and suggest that it may be involved in relevant ET pathways and genes.

Introduction

Essential tremor (ET) is one of the most common movement disorders and is typically characterized by a kinetic tremor in the hand or arms[1]. The severity tends to increase with age and may involve different regions such as the head, voice or jaw[2]. Previous studies investigating the histology of post-mortem tissue have pinpointed the cerebellum as a region of interest for ET[3]. Specifically, abnormalities with Purkinje cell axons and dendrites were found in ET brains[4]. Furthermore, the olivocerebellar circuitry has been implicated in ET pathology and many calcium voltage channels are highly expressed in this circuitry[5].

The genetic etiology of ET has remained largely elusive and most studies have focused on common or rare variants and on looking for genetic overlap with other disorders[6,7]. Twin studies have shown that ET has a concordance of 69–93% in monozygotic twins and 27–29% in dizygotic twins, which suggests that both genetic and environmental factors drive the onset and development of this complex trait[8]. A recent genome-wide association study (GWAS) identified a significant locus in *STK32B* and found that ET patients overexpressed *STK32B* in cerebellar tissue by comparison to healthy controls[9]. *STK32B* is transcribed and translated into YANK2, a serine/threonine kinase, that has not been well characterized. There have been several exome-wide studies that implicated different genetic variants as causes of ET. The first ET-implicated gene found through exome

sequencing was the Fused in Sarcoma gene (*FUS*)[10]. However, it is unclear whether these "ET" genes interact or have indirect effects on the expression of each other.

To understand the effects of overexpressed *STK32B* and identify pathways potentially relevant to ET, we overexpressed the gene in human cerebellar DAOY cells and compared transcriptomic changes in overexpressed cells and empty-vector controls using RNA sequencing. Several interesting pathways such as axon guidance, calcium ion transmembrane transport, and olfactory transduction were significantly enriched after overexpression of *STK32B*. We also identified previously implicated ET genes whose expression is dysregulated through the overexpression of *STK32B*, suggesting that overexpressed *STK32B* may have relevant downstream effects.

Results

Confirming overexpression of *STK32B* (YANK2 protein)

The *STK32B* stable cell lines had higher protein expression of YANK2, which was detected by Western blot (Supplementary Figure 1–2). RNA sequencing (RNA-Seq) confirmed that the stable cell lines have higher *STK32B* RNA levels compared to controls; it was the most significantly differentially expressed gene (Figure 1–2).

Quality control of RNA-seq analyses

The QQ-plot for differentially expressed genes did not show stratification or potential biases (Supplementary Figure 3). The M-A plot showed slight enrichment of downregulated genes compared to upregulated genes (Supplementary Figure 4). A principal component (PC) plot showed separation of controls and *STK32B* cell lines (Figure 3). Additionally, the dendrogram with heatmap shows that controls and *STK32B* cell lines are distinct (Supplementary Figure 5). The mean-variance plot shows the shrinkage under the sleuth model (Supplementary Figure 6).

Overexpression of *STK32B* affects expression of previously identified ET-associated genes

A total of 3,794 genes were found to be differentially expressed with a q-value <0.05. There were 425 genes with a $\beta > |0.5|$ and q-value <0.05. Amongst the 425 genes, three potentially relevant ET genes were dysregulated: *FUS* (q-value = 0.007, β=0.812) and two calcium voltage channel genes that are enriched in the olivocerebellar circuitry, *CACNA1C* (q-value = 0.011, β= 0.503) and

CACNA1A (q-value = 0.030, β= 0.702). Several pathways and gene ontologies were enriched for differentially expressed genes (DEGs) due to the overexpression of *STK32B*, including olfactory transduction (P=2.68E-39), axon guidance (P=9.50E-36), and calcium ion transmembrane transport (P=3.02E-31) (Table 1).

Gene network analyses

To identify which cluster of DEGs drove the significant pathways, gene network analysis based on co-expression was done and identified 14 different clusters within the differentially expressed genes (Figure 4). Analysis of the top 3 largest clusters for pathway enrichments found several similar pathways in different databases including axon guidance (P<1.09E-12) in cluster 1 and calcium signalling pathway in cluster 3 (2.06E-05).

Discussion

The genetic etiology of ET is complex and likely explained by a combination of copy number variants, rare variants, gene-gene interactions and common variant drivers. One of the most significantly enriched pathways we identified was olfactory signalling and transduction. Previous reports have shown conflicting evidence about olfactory loss in ET[11,12]. It may be that ET patients with dysregulated olfactory signalling have overexpressed *STK32B*, which may contribute to the subset of ET patients with olfactory loss.

Interestingly, *FUS* was amongst the genes dysregulated when *STK32B* was overexpressed. In the exome familial ET study that identified *FUS*, we also found reduced mRNA levels for *FUS*[10]. Similarly, the expression of *FUS* is lower when *STK32B* is overexpressed, suggesting an indirect relationship between the two genes. Additionally, two calcium voltage-gated channel genes, *CACNA1C* AND *CACNA1A* were overexpressed. Enrichment analyses found calcium ion transmembrane transport to be highly significant in GO Processes, suggesting that *STK32B* may play a role upstream of these genes. In the olivocerebellar circuitry, a system implicated in ET, is enriched for both of these genes[5,13]. *CACNA1A* has been shown to be predominantly expressed in Purkinje cells, a cell type relevant to ET[13]. Another enriched pathway was axon guidance. A previous study identified the *TENM4* missense variant segregating within ET families[14]. *TENM4* is a regulator of axon guidance and myelination and Tenm4 knockout mice showed an ET

116 phenotype, suggesting that axon guidance is important in ET[14]. Similarly, overexpressed *STK32B*
117 could be dysregulating important pathways relevant to axon guidance.
118
119 By sub-stratifying the overexpressed genes into different clusters that are co-expressed, several
120 interesting pathways involving the cardiovascular system were identified. Pathways such as right
121 ventricular cardiomyopathy in KEGG and angiogenesis in GO Processes were found among the
122 top five significant pathways. In certain ET patients, beta-blockers can reduce tremor magnitude
123 and frequency. Beta-blockers lower blood pressure and are used to treat irregular heart rhythm and
124 other cardiovascular phenotypes. A common treatment for ET is propranolol, a beta-blocker. This
125 was a drug developed for cardiovascular health that affects adrenergic activity, but still reduces
126 tremor in ET individuals. This could suggest that overexpressed *STK32B* affects cardiovascular
127 health, which may in turn affect or lead to the ET phenotype or that *STK32B* may be pleiotropic
128 and affect the nervous and cardiovascular system differently.
129
130 Due to the heterogeneity of ET, it is likely that not all ET-affected individuals have overexpression
131 of *STK32B*. One limitation of this study is that DAOY cells are a cancerous cell line and may not
132 be the ideal model for understanding the transcriptome of Purkinje cells. Future studies on the
133 effects of *STK32B* overexpression could use induced pluripotent stem cells differentiated into cells
134 with Purkinje cells properties; such cells would likely have less biological noise. However, our
135 findings support the idea that *STK32B* is a gene of interest for a subset of ET cases, and further
136 investigations into how *STK32B* may interact with other genes are warranted.
137

138 Methods and Materials

139 Cell Culture and plasmid construction

140 The DAOY cell line was cultured in Eagle's Minimum Essential Medium (EMEM) with 10% fetal
141 bovine serum (FBS) at 37 degrees Celsius and 5% CO_2 with the Glico Pen-Strep-Glutamine
142 cocktail at 1X. Cells were passaged every 2 days at 80-90% confluence and at the same time. The
143 cDNA of *STK32B* (NM_001306082.1) was inserted into a pcDNA3.1(+) vector containing a
144 neomycin resistance gene, used as a selectable marker. This transcript was picked because it had
145 the highest expression in the cerebellum based on GTEx 53 v7. The plasmid was transformed and

146 expanded in XL10-Gold *Escherichia coli* strain (Stratagene). The cDNA of the plasmid was sent
147 for Sanger sequencing to validate the gene sequence.
148

149 ## Transfection and deriving stable cell lines

150 The cells were transfected for 48 hours with 8 ug of DNA of using the jetPRIME transfection
151 reagent (Polyplus). A green fluorescent protein (GFP) control vector was used to assess and
152 estimate transfection efficiency and optimize transfection parameters. Stable cell lines were
153 established by subjecting transfected cells to G418 antibiotic at 1 μg/mL for 10 days and maintained
154 at a concentration of 400 μg/mL for an additional 2 weeks. A kill curve was done to determine the
155 ideal antibiotic selection. In parallel, empty pcDNA3.1(+) vector control lines were also grown and
156 underwent antibiotic selection.
157

158 ## Quantifying protein expression

159 Protein extraction was done from whole cell lysate using a custom buffer made of SDS, urea and
160 β-mercaptomethanol. Protein concentrations were measured using both a Bradford Assay. Protein
161 extracts were run on a 12% polyacrylamide gel for 1 hour and transferred to a PVDF membrane
162 with a BioRad X Trans-Blot Turbo Transfer System for 30 minutes. The membrane was blocked
163 with a 5% fat-free milk and PBS-tween-20 solution for one hour. After, the membrane was
164 incubated in a new 5% fat-free milk solution with an added anti-rabbit primary YANK2 antibody
165 at a concentration of 1:1,000 overnight. The membrane was then washed 3 times with PBS-tween
166 for 10 minutes each. The membrane was then incubated with a secondary antibody, anti-donkey
167 HCP at a concentration of 1:20,000 for one hour. The membrane was washed 3 times with PBS-
168 tween for 10 minutes each. The BioRad Western ECL substrate was added to the membrane. The
169 Western blot was imaged using the BioRad ChemiDoc Touch Imaging System. Next, the
170 membrane was stripped using the Restore Western Blot Stripping Buffer (ThermoFisher Scientific)
171 and blocked with 5% fat-free milk-PBS tween-20 solution for 1 hour. The membrane was incubated
172 with anti-mouse Actin antibody at a concentration of 1:5,000 overnight. The membrane was washed
173 3 times with PBS-tween for 10 minutes each. Next, the membrane was incubated with anti-goat
174 HCP at a concentration of 1:20,000 for 1 hour. The membrane was washed 3 times with PBS-tween
175 for 10 minutes each and reimaged using the BioRad Western ECL substrate and BioRad ChemiDoc
176 Touch Imaging System. The top three overexpressed *STK32B* cell lines were determined by
177 densitometry and selected for RNA sequencing.

178

179 ## RNA extraction and sequencing

180 RNA was extracted using the RNeasy Mini Kit (Qiagen). The RNA concentration was measured
181 using the Synergy H4 microplate reader. RNA for the top three overexpressed *STK32B* cell lines
182 and three empty-vector controls was sent to Macrogen Inc. for sequencing. Library preparation
183 was done with the TruSeq Stranded Total RNA Kit (Ilumina) with Ribo-Zero depletion.
184 Sequencing was done on the NovaSeq 6000 at 150bp paired-end reads with a total of 200M reads.
185 Samples were randomized for cell lysis, RNA extraction, Ribo-Zero depletion, library preparation
186 and sequencing to account for potential batch effects.

187

188 ## Data processing and quality control

189 The FASTQ files were pseudo-aligned with Salmon using the Ensembl v94 annotation of the
190 human genome[16]. The parameters of Salmon included the following: 200 bootstraps with mapping
191 validation, GC bias correction, sequencing bias correction, 4 range factorization bins, a minimum
192 score fraction of 0.95 and VB optimization with a VB prior of 1e-5. The estimated counts were
193 analyzed using sleuth to identify DEGs[17]. A likelihood ratio test was used to identify differentially
194 expressed transcripts and a Wald test was used to get β values ($\log_2(x + 0.5)$). Additionally,
195 transcript-level aggregation was done against the Ensembl v94 annotation to determine gene-level
196 differential expression. P-values were corrected using the Benjamini-Hochberg procedure to
197 account for false discovery rate (FDR). Q-value (p-values corrected for FDR) significance was set
198 for an FDR of <0.05. A principal component (PC) plot and heatmap was done to identify clusters.

199

200 ## Pathway and gene set enrichment analysis

201 Pathway and gene set enrichment for relevant databases was done using Gene Network 2.0. To
202 investigate genes with larger fold changes, only differentially expressed genes with a $\beta > |0.5|$ were
203 analyzed for pathway enrichments. Network clustering was done by grouping genes based on co-
204 expression. Pathway analyses were also conducted with Gene Network 2.0 for the clusters using a
205 Wilcoxin test.

206

References

1. Elble, R. J. What is Essential Tremor? *Curr. Neurol. Neurosci. Rep.* **13,** 353 (2013).
2. Haubenberger, D. & Hallett, M. Essential Tremor. *N. Engl. J. Med.* **378,** 1802–1810 (2018).
3. Gironell, A. The GABA Hypothesis in Essential Tremor: Lights and Shadows. *Tremor Other Hyperkinet. Mov. (N. Y).* **4,** 254 (2014).
4. Axelrad, J. E. *et al.* Reduced Purkinje cell number in essential tremor: a postmortem study. *Arch. Neurol.* **65,** 101–7 (2008).
5. Schmouth, J.-F., Dion, P. A. & Rouleau, G. A. Genetics of essential tremor: From phenotype to genes, insights from both human and mouse studies. *Prog. Neurobiol.* **119–120,** 1–19 (2014).
6. Liao, C. *et al.* Investigating the association and causal relationship between restless legs syndrome and essential tremor. *Parkinsonism Relat. Disord.* (2018). doi:10.1016/j.parkreldis.2018.10.022
7. Houle, G. *et al.* Teneurin transmembrane protein 4 is not a cause for essential tremor in a Canadian population. *Mov. Disord.* **32,** 292–295 (2017).
8. Tanner, C. M. *et al.* Essential tremor in twins: an assessment of genetic vs environmental determinants of etiology. *Neurology* **57,** 1389–91 (2001).
9. Müller, S. H. *et al.* Genome-wide association study in essential tremor identifies three new loci. *Brain* **139,** 3163–3169 (2016).
10. Merner, N. D. *et al.* Exome Sequencing Identifies FUS Mutations as a Cause of Essential Tremor. *Am. J. Hum. Genet.* **91,** 313–319 (2012).
11. Applegate, L. M. & Louis, E. D. Essential tremor: Mild olfactory dysfunction in a cerebellar disorder. *Parkinsonism Relat. Disord.* **11,** 399–402 (2005).
12. Shah, M., Muhammed, N., Findley, L. J. & Hawkes, C. H. Olfactory tests in the diagnosis of essential tremor. *Parkinsonism Relat. Disord.* **14,** 563–568 (2008).
13. Mori, Y. *et al.* Primary structure and functional expression from complementary DNA of a brain calcium channel. *Nature* **350,** 398–402 (1991).
14. Hor, H. *et al.* Missense mutations in TENM4 , a regulator of axon guidance and central myelination, cause essential tremor. *Hum. Mol. Genet.* **24,** 5677–5686 (2015).
15. Kim, J., Basak, J. M. & Holtzman, D. M. The role of apolipoprotein E in Alzheimer's disease. *Neuron* **63,** 287–303 (2009).
16. Patro, R., Duggal, G., Love, M. I., Irizarry, R. A. & Kingsford, C. Salmon provides fast and bias-aware quantification of transcript expression. *Nat. Methods* **14,** 417–419 (2017).
17. Pimentel, H., Bray, N. L., Puente, S., Melsted, P. & Pachter, L. Differential analysis of RNA-seq incorporating quantification uncertainty. *Nat. Methods* **14,** 687–690 (2017).

Figures and Tables

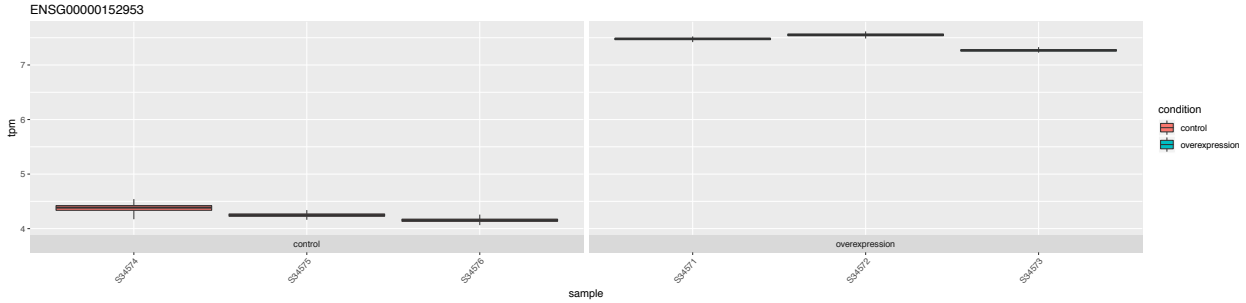

Figure 1. The RNA expression of *STK32B* overexpressed cells compared to empty-vector controls based on RNA sequencing data. Error bars show the technical variance determined with 200 bootstraps. Abbreviations: TPM, transcript per million.

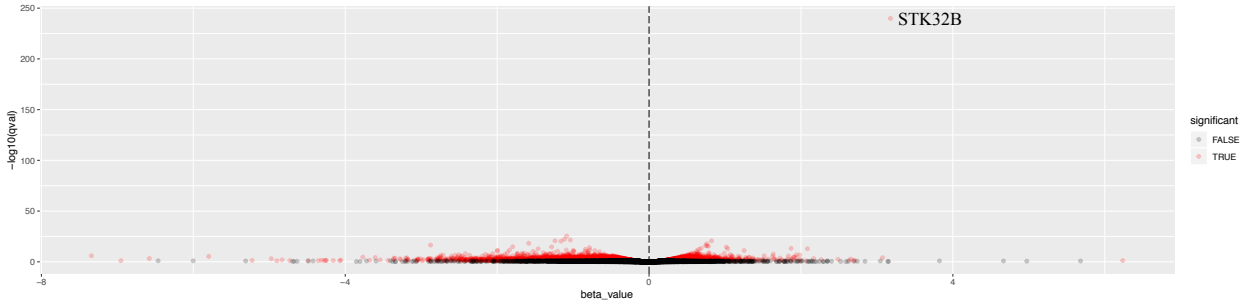

Figure 2. Volcano plot of comparing overexpressed *STK32B* to empty-vector controls. Differentially expressed genes ($q < 0.05$) are shown in red. Beta value was determined with a Wald's test.

Figure 3. Principle component analysis plot of RNA sequencing data of *STK32B* overexpressed cells and empty-vector controls. Overexpressed cells shown in blue and controls shown in red.

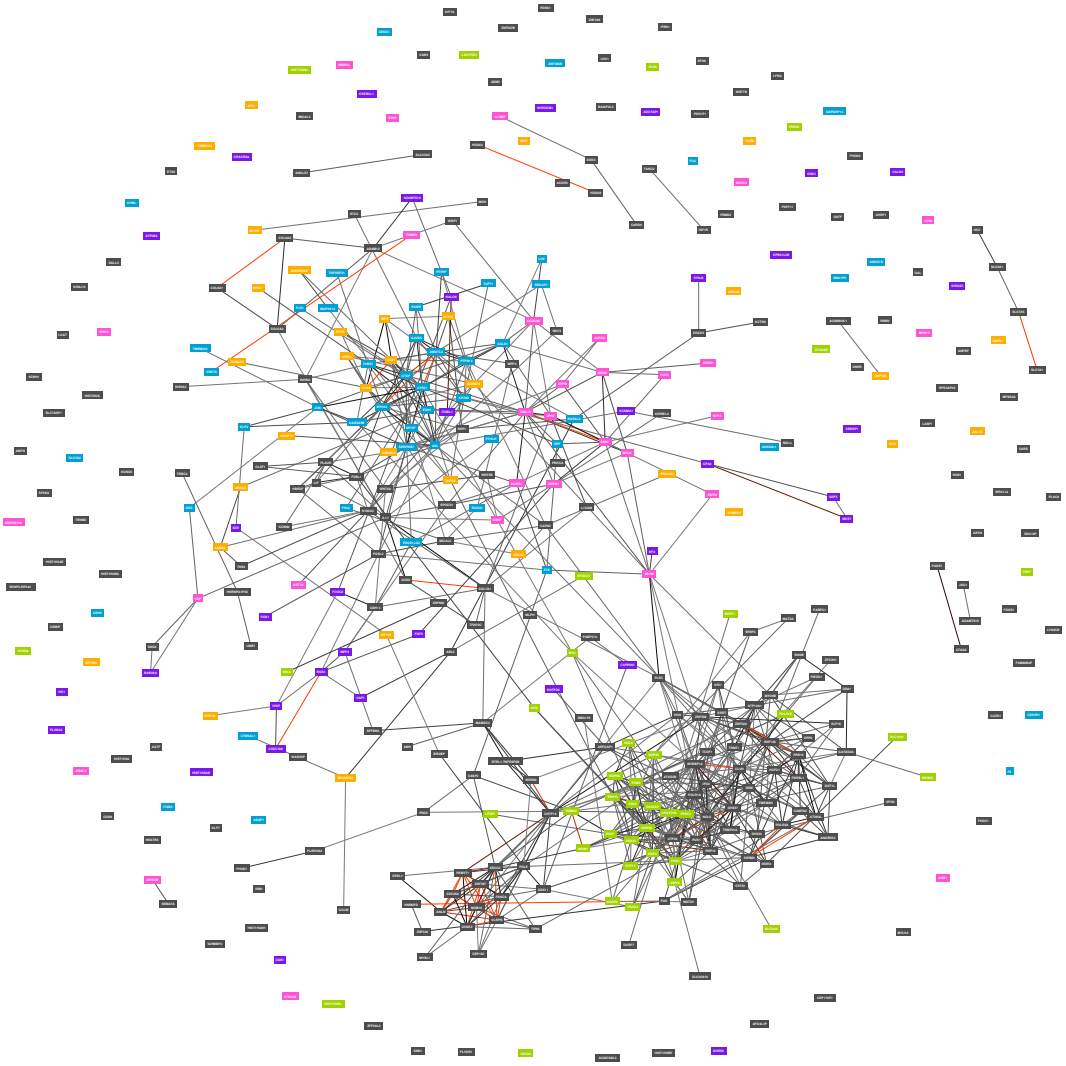

Figure 4. Gene network of differentially expressed genes based on co-expression of RNA sequencing data for 31,499 samples. Each unique colour represents a cluster.

277 **Table 1. Gene ontology and pathway analyses of differentially expressed genes.**

Gene Set ID	Gene Set Name	*P*	Database
KEGG_OLFACTORY_TRANSDUCTION	Olfactory transduction	2.68E-39	KEGG
KEGG_PATHWAYS_IN_CANCER	Pathways in cancer	2.96E-28	
KEGG_FOCAL_ADHESION	Focal adhesion	1.19E-26	
KEGG_BLADDER_CANCER	Bladder cancer	6.53E-25	
KEGG_ECM_RECEPTOR_INTERACTION	Ecm-receptor interaction	8.38E-25	
GO:0001650	fibrillar center	1.13E-29	GO Cellular
GO:0031012	extracellular matrix	8.57E-27	
GO:0001725	stress fiber	1.24E-26	
GO:0005925	focal adhesion	2.82E-23	
GO:0015629	actin cytoskeleton	4.02E-22	
REACTOME:R-HSA-381753	Olfactory Signaling Pathway	3.22E-46	Reactome
REACTOME:R-HSA-418555	G alpha (s) signalling events	1.19E-29	
REACTOME:R-HSA-3000170	Syndecan interactions	1.53E-27	
REACTOME:R-HSA-2022090	Assembly of collagen fibrils and other multimeric structures	4.31E-25	
REACTOME:R-HSA-1474290	Collagen formation	2.35E-24	
GO:0050911	detection of chemical stimulus involved in sensory perception of smell	1.00E-44	Go Processes
GO:0007411	axon guidance	9.50E-36	
GO:0048146	positive regulation of fibroblast proliferation	1.31E-33	
GO:0070588	calcium ion transmembrane transport	3.02E-31	
GO:0050907	detection of chemical stimulus involved in sensory perception	3.14E-31	

278

279

280

281 **Table 2. Gene ontology and pathway analyses of differentially expressed gene for the three largest clusters based on co-**
282 **expression.**

Gene Set Name	P	Database	Cluster
Regulation of actin cytoskeleton	1.03E-13	KEGG	1
Pathways in cancer	1.23E-13		
Axon guidance	1.09E-12		
Focal adhesion	4.96E-12		
Arrhythmogenic right ventricular cardiomyopathy (ARVC)	4.63E-09		
fibrillar center	1.13E-29	GO Cellular	
extracellular matrix	8.57E-27		
stress fiber	1.24E-26		
focal adhesion	2.82E-23		
actin cytoskeleton	4.02E-22		
actin binding	3.66E-15	GO Function	
laminin binding	2.37E-13		
insulin-like growth factor binding	9.72E-13		
collagen binding	3.73E-12		
protein heterodimerization activity	5.54E-12		
cell migration involved in sprouting angiogenesis	7.07E-18	GO Processes	
cell migration	2.94E-16		
inactivation of MAPK activity	3.31E-15		
cytoskeleton organization	6.34E-15		
negative regulation of cell migration	9.12E-15		
Cell-extracellular matrix interactions	7.16E-15	Reactome	
Signal Transduction	1.98E-13		
Non-integrin membrane-ECM interactions	2.58E-12		
Signaling by Rho GTPases	1.84E-11		

EPHA-mediated growth cone collapse	2.30E-11		
Rna polymerase	4.57E-13	KEGG	2
Pyrimidine metabolism	1.37E-12		
Alzheimer's disease	3.55E-11		
Purine metabolism	4.11E-11		
Gnrh signaling pathway	1.84E-09		
nucleolus	5.96E-19	GO Cellular	
preribosome, large subunit precursor	2.21E-18		
small-subunit processome	5.13E-18		
DNA-directed RNA polymerase III complex	5.10E-15		
DNA-directed RNA polymerase I complex	1.85E-14		
pseudouridine synthase activity	7.75E-16	GO Function	
RNA binding	1.25E-15		
snoRNA binding	4.90E-14		
rRNA binding	3.55E-13		
ATP-dependent RNA helicase activity	5.23E-13		
RNA secondary structure unwinding	1.57E-16	GO Processes	
tRNA modification	7.73E-16		
positive regulation of gene expression, epigenetic	3.09E-15		
ribosomal large subunit biogenesis	3.17E-15		
maturation of SSU-rRNA from tricistronic rRNA transcript (SSU-rRNA, 5.8S rRNA, LSU-rRNA)	3.32E-15		
rRNA modification in the nucleus and cytosol	3.38E-18	Reactome	
tRNA processing	1.65E-17		
tRNA modification in the nucleus and cytosol	1.66E-16		
rRNA processing	9.91E-15		
tRNA processing in the nucleus	1.69E-14		
RIG-I-like receptor signaling pathway	1.24E-10	KEGG	

Cytosolic DNA-sensing pathway	1.92E-07		
O-glycan biosynthesis	1.163E-06		
Focal adhesion	1.36893E-06		
Calcium signaling pathway	2.06986E-05		
caveola	2.00E-08	GO Cellular	
proteinaceous extracellular matrix	7.41E-08		
postsynaptic membrane	2.45E-06		
microfibril	4.99E-06		
extracellular matrix	1.12E-05		3
type I interferon receptor binding	3.64E-07	GO Function	
neuropeptide binding	5.89E-07		
scavenger receptor activity	6.23E-07		
calcium-dependent phospholipid binding	9.44E-07		
RNA binding	2.46E-06		
response to mechanical stimulus	8.42E-09	GO Processes	
lung development	1.55E-08		
negative regulation of neuron apoptotic process	5.29E-08		
cellular response to hypoxia	7.29E-08		
regulation of type I interferon-mediated signaling pathway	1.11E-07		
O-glycosylation of TSR domain-containing proteins	3.73E-10	Reactome	
Defective B3GALTL causes Peters-plus syndrome (PpS)	5.15E-10		
DDX58/IFIH1-mediated induction of interferon-alpha/beta	1.29E-09		
O-linked glycosylation	4.91E-08		
Diseases associated with O-glycosylation of proteins	1.04E-07		